

UNIVERSITY UTRECHT

BACHELOR RESEARCH

---

# Quadrupole modes in a cold Bose-gas

---

*Author:*

Maikel DOORNHEIN

*Supervisor:*

Dr. Peter van der  
STRATEN

February 10, 2014

# Contents

|          |                                |           |
|----------|--------------------------------|-----------|
| <b>1</b> | <b>Introduction</b>            | <b>2</b>  |
| <b>2</b> | <b>Theory</b>                  | <b>5</b>  |
| 2.1      | Collisionless Regime . . . . . | 8         |
| 2.2      | Hydrodynamic Regime . . . . .  | 9         |
| 2.3      | Intermediate Regime . . . . .  | 11        |
| <b>3</b> | <b>Experiment</b>              | <b>14</b> |
| 3.1      | Measuring . . . . .            | 14        |
| 3.2      | Analysis . . . . .             | 18        |

# 1 Introduction

The goal of this paper is to study the hydrodynamic properties of a very cold bose-gas. Our main focus will be the behavior of quadrupole oscillations in a so called thermal cloud. With a thermal cloud we mean throughout the text a collection of very cold atoms in a cylindrical symmetric shape that is nonetheless too warm to be a (partial) Bose-Einstein condensate. How the atoms that make up the cloud are trapped and cooled has been described many times before and it is of no interest to both writer and reader to repeat this once more. We only remark that curious readers can find the procedure in Kollers thesis [1].

The particles we are using are  $^{23}\text{Na}$ .  $^{23}\text{Na}$  is a boson composed of fermions and therefore it must have an integer value for the total spin. Neutral atoms consist of an equal number of protons and electrons and therefore the statistics that the atom obeys is completely determined by the number of neutrons. An even number of neutrons makes it behave as a boson while an odd number results in a fermion.

Inside a magnetic field hyperfine splitting occurs due to the coupling of the nuclear spin ( $I = \frac{3}{2}$  for  $^{23}\text{Na}$ ) to the total electronic angular momentum ( $J = \frac{1}{2}$ ). This results in two possible values for the total angular momentum ( $F = I \pm J$ ). We thus find the groundstate  $F = 1$  and the excited state  $F = 2$ . For  $F = 1$  there are 3 different values for the magnetic quantum number  $m_f$  namely  $-1 \leq m_f \leq 1$  in integer steps. For  $F = 2$  there are 5 different values  $-2 \leq m_f \leq 2$  in integer steps.

At the beginning of our experiment, after the trapping and cooling processes, the  $^{23}\text{Na}$  atoms in the thermal cloud are trapped in a harmonic magnetic potential. All atoms are in the ground-state  $F = 1$ . Therefore about one third of the atoms has  $m_f = 0$  and consequently are not effected by a magnetic trap. These atoms are thus lost. The same is valid for atoms with  $m_f = 1$  for these seek a maximum in the magnetic potential, which is absent. These atoms are accelerated away from the minimum in the harmonic potential. We are left with atoms that have quantum numbers  $F = 1$  and  $m_f = -1$ . The trap potential is then given by

$$V(r) = \frac{1}{2}(\omega_x^2 x^2 + \omega_y^2 y^2 + \omega_z^2 z^2) = \frac{1}{2}m(\omega_\rho^2 \rho^2 + \omega_z^2 z^2) \quad (1)$$

Where we express the cylindrical symmetry of the trap ( $\omega_x = \omega_y = \omega_\rho$ ) by introducing the radial coordinate  $\rho^2 = x^2 + y^2$ . The z-direction will sometimes be referred to as the axial direction.  $\omega$  is the frequency with which the particles oscillate from one side to the other in a given direction. Logically this frequency is smaller in the direction where the dimensions of the cloud are longer.

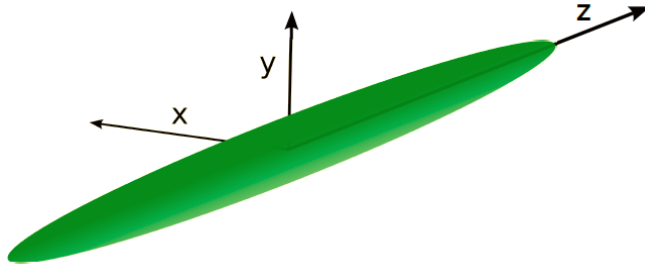


**Figure 1:** The used coordinate system. Notice the cylindrical symmetry of the cigar shaped cloud.

Above the critical temperature  $T_c$  we can use the high temperature limit of the Bose-distribution for the density distribution of the particles [5]

$$n(r) = \frac{N}{2\pi^{\frac{3}{2}}\sigma_\rho^2\sigma_z} \text{Exp}\left[-\frac{\rho^2}{2\sigma_\rho^2} - \frac{z^2}{2\sigma_z^2}\right] \quad (2)$$

Here  $\sigma_\rho$  and  $\sigma_z$  are the widths of the gaussian distribution that depend on the temperature and on the trapping frequencies.

$$\sigma_\rho = \sqrt{\frac{K_b T}{m\omega_\rho^2}} \quad \sigma_z = \sqrt{\frac{K_b T}{m\omega_z^2}} \quad (3)$$

This shows that the width of the cloud in a given direction is inversely proportional to the trapping frequency in that direction. The density distribution is easily derived by normalizing the Boltzmann distribution



$$P(r) \propto \text{Exp}-\frac{V(r)}{K_b T} \quad (4)$$

and multiplying by the number of atoms  $N$ . The shape of the cloud is determined by the trapping frequencies as mentioned above. We now introduce a parameter that describes this shape.

$$\lambda = \frac{\omega_{rad}}{\omega_{ax}} \quad (5)$$

We call this the aspect ratio. It is not uncommon in scientific papers treating quadrupole modes to use the inverse aspect ratio which is then also indicated with  $\lambda$ . This can be confusing but it will be clearly stated when this definition is used. Figure 2 shows what an actual quadrupole mode in a cigar shaped cloud looks like.

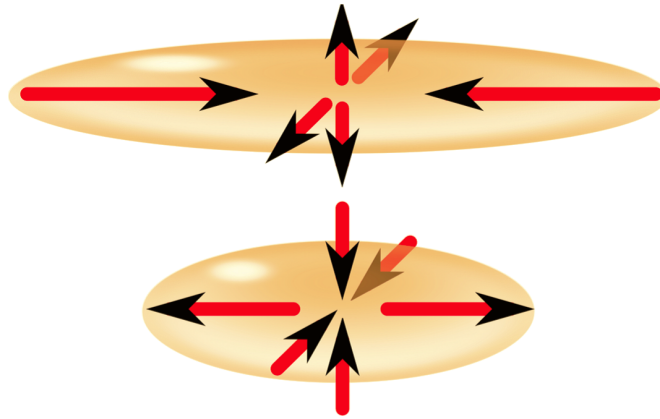


**Figure 2:** In the top picture the cloud is fully stretched in the axial direction and fully compressed in the radial direction. Below it is the other way around. If (not in this picture) the axial direction becomes smaller than the radial direction the cloud assumes a "pancake"-like shape

From our discussion above it is not hard to see that the expected quadrupole frequencies are either

$$\omega_q = 2\omega_z \quad \text{or} \quad \omega_q = 2\omega_\rho \quad (6)$$

depending on what mode is excited. This result is only correct if the atoms are treated like point particles that do not interact with one another.

## 2 Theory

In the previous section it was mentioned that, in the case the atoms do not interact with each other, the two possible quadrupole modes of the cloud are simply twice the axial and the radial trapping frequencies. It turns out however that interactions between the particles modify the quadrupole modes. The first theoretical treatment of this phenomenon was given by Stringari et al. [2]. They investigated the behaviour of the quadrupole modes in the regime where the phase-space distribution function

$$f(\vec{r}, \vec{p}, t) = \left( \frac{e^{\frac{(\vec{p} - m\vec{v}(\vec{r}, t))^2}{2m} - \mu(\vec{r}, t)}}{K_b T(\vec{r}, t)} - 1 \right)^{-1} \quad (7)$$

is in local thermal equilibrium. This is a valid assumption when there are frequent collisions between the atoms. In other words the collision rate must be high. We call this the hydrodynamic regime. By making this assumption they predicted the quadrupole modes to be

$$\omega_q^2 = \frac{\omega_\rho^2}{3} (5 + 4\lambda^2 \pm \sqrt{25 + 16\lambda^4 - 32\lambda^2}) \quad (8)$$

in the fully hydrodynamic regime. In current experiments however it is challenging even to achieve a density high enough to get close to the intermediate regime, where the cloud is neither approximately collisionless nor hydrodynamic. One might say that the density, and thus the number of collisions, is easily increased

by just increasing the trap strength. Assuming you can generate the stronger magnetic field to accomplish this it will not necessarily cause more collisions. To understand this we must keep in mind that the higher the density the greater the chance of losing an atom due to 3-body interaction. Losing atoms in this way decreases the density we initially raised. Furthermore the temperature will increase when compressing the cloud. It will turn out that this also causes the collision rate to decrease. To increase the number of collisions we must balance these effects.

We thus need a theoretical prediction for this intermediate regime in order to compare experiment and theory. In later years this theory was realized in the same way by two different groups [3, 4]. Both papers approach the subject by considering the evolution of the phase-space distribution when they added a collisional term to the Boltzmann equation

$$\frac{\partial f}{\partial t} + \vec{v}_1 \cdot \nabla_r f - \frac{\nabla V(\vec{r})}{m} \cdot \nabla_{v_1} f = I_{coll}[f] \quad (9)$$

Where the collisional term is given by

$$I_{coll}[f] = \frac{\sigma_0}{4\pi} \int |\vec{v}_2 - \vec{v}_1| (f(\vec{v}_1') f(\vec{v}_2') - f(\vec{v}_1) f(\vec{v}_2)) d^2\omega d^3v_2 \quad (10)$$

In short this integral describes the collision between particles 1 and 2 such that  $v_1' \rightarrow v_1$  and  $v_2' \rightarrow v_2$ . The average of a function that depends on one or both of the variables  $r$  and  $v$  can be calculated by using the phase-space density distribution function  $f(r,p,t)$

$$\langle \chi \rangle = \frac{1}{N} \int \chi(\vec{r}, \vec{p}) f(\vec{r}, \vec{p}, t) d^3r d^3v \quad (11)$$

How this quantity evolves in time can be derived from the Boltzmann equation with the collisional term given by Equation (10). It is shown to be

$$\frac{d \langle \chi \rangle}{dt} = \langle \vec{v} \cdot \nabla_r \chi \rangle + \left\langle \frac{\nabla V(\vec{r})}{m} \cdot \nabla_v \chi \right\rangle = \langle \chi I_{coll} \rangle \quad (12)$$

Consequently they insert different  $\chi$ 's (for example  $\chi = v^2$ ) and thereby acquire a coupled system of equations. Most of the collisional terms turn out to be zero, but one of them does not. The coupled equations yield the desired result, a dispersion relation which takes the following form

$$(\omega_q^2 - 4\omega_z^2)(\omega_q^2 - 4\omega_\rho^2) - \frac{1}{\omega_q\tau}[\omega_q^4 - \frac{2}{3}\omega_q^2(5\omega_\rho^2 + 4\omega_z^2) + 8\omega_\rho^2\omega_z^2] = 0 \quad (13)$$

This is the full dispersion relation of a classical gas in a harmonic trap. Here

$$\tau = \frac{5}{4\gamma_{coll}} \quad (14)$$

With

$$\gamma_{coll} = \frac{n(0)v_{th}\sigma_0}{2} \quad (15)$$

Where  $n(0)$  stands for the density of the Gaussian distribution at the center.

$$v_{th} = \sqrt{\frac{8K_bT}{\pi m}} \quad (16)$$

And  $\sigma_0 = 8\pi a^2$  the collisional cross section of sodium. We take  $a = 2.80$  nm the s-wave scattering length of a sodium atom. It can be shown that  $\gamma_{coll}$  can also be expressed in the number of atoms

$$\gamma_{coll} = \frac{Nm\sigma_0\omega_{rad}\omega_{ax}}{2\pi^2 K_b T} \quad (17)$$

With  $N$  the total number of particles and  $m$  the mass of a single particle.  $K_b$  is the Boltzmann constant and  $T$  the temperature of the cloud. It is more intuitively convenient however to express the hydrodynamicity as:

$$\tilde{\gamma} = \frac{\gamma}{\omega_{ax}} \quad (18)$$

This represents the mean number of times a particle interacts with another particle during one oscillation in the axial direction. The full dispersion relation can be rewritten only in terms of the aspect ratio and the hydrodynamicity parameter as will be shown later on.

## 2.1 Collisionless Regime

The full dispersion relation calculated for the intermediate regime

$$(\omega_q^2 - 4\omega_z^2)(\omega_q^2 - 4\omega_\rho^2) - \frac{1}{\omega_q\tau}[\omega_q^4 - \frac{2}{3}\omega_q^2(5\omega_\rho^2 + 4\omega_z^2) + 8\omega_\rho^2\omega_z^2] = 0 \quad (19)$$

can be taken in two different limits. When we let the collision time  $\tau$  go to infinity (in practice  $\omega_q\tau \rightarrow \infty$ ) it reduces to the dispersion relation corresponding to the collisionless regime

$$(\omega_q^2 - 4\omega_z^2)(\omega_q^2 - 4\omega_\rho^2) \quad (20)$$

which has the solutions

$$\omega_q = 2\omega_z \quad \omega_q = 2\omega_\rho \quad (21)$$

Confirming our less mathematical presumption at the beginning of the first section. Because we aim to compare different situations to the collisionless regime it is convenient to normalize the solutions to the axial trap frequency  $\omega_z$ . The normalized solutions are indicated with  $\omega_t = \frac{\omega_q}{\omega_z}$

$$\omega_t = 2\frac{\omega_z}{\omega_z} = 2 \quad \omega_t = 2\frac{\omega_\rho}{\omega_z} = \frac{2}{\lambda} \quad (22)$$

When we plot the solutions as a function of the inverse aspect ratio  $\lambda^{-1}$  the following graph is obtained

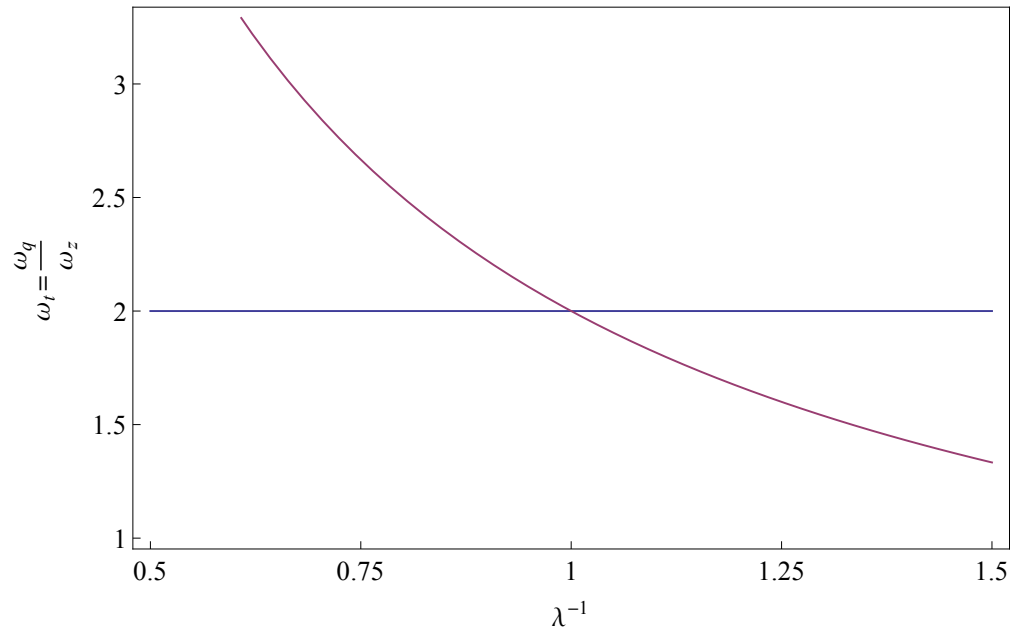


**Figure 3:** We observe a crossing of the two modes at  $\lambda = 1$ . This means that the modes are degenerate when the thermal cloud is perfectly round before the kick.

## 2.2 Hydrodynamic Regime

In the hydrodynamic regime collisions between the atoms dominate. This is represented in the full dispersion relation by taking the limit of the collision time going to zero ( $\omega_q \rightarrow 0$ ). We obtain

$$\omega_q^4 - \frac{2}{3}\omega_q^2(5\omega_\rho^2 + 4\omega_z^2) + 8\omega_\rho^2\omega_z^2 = 0 \quad (23)$$

By some rewriting it is possible to attain the original result for a hydrodynamic bose-gas

$$\omega_q^2 = \frac{\omega_\rho^2}{3} (5 + 4\lambda^2 \pm \sqrt{25 + 16\lambda^4 - 32\lambda^2}) \quad (24)$$

We thus obtain, as required, the correct solutions from the intermediate dispersion relation in both cases by taking the two different limits for the collision time. We normalize the solutions in the same way as before and plot them as a function of  $\lambda$

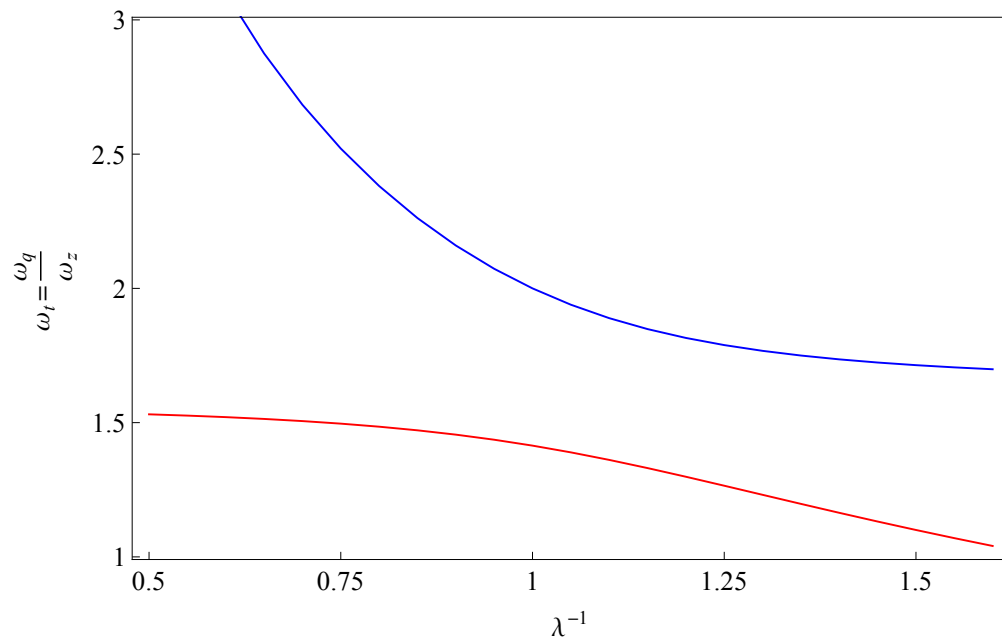


**Figure 4:** This time we observe that the two frequencies do not cross in the vicinity of  $\lambda = 1$ . Instead they display an avoided crossing which indicates two coupled modes.

As we pointed out above however we are mainly interested in the behavior of the modes in the intermediate regime. In order to make the plot above for hydrodynamicities other than the two limits we addressed before it is necessary to solve the dispersion relation numerically. This will be the subject of the next paragraph.

## 2.3 Intermediate Regime

Because our experiments take place in the intermediate regime we want to solve the dispersion relation numerically for arbitrary hydrodynamicity and aspect ratio. We begin by introducing  $\omega_t = \frac{\omega_q}{\omega_z}$  and the inverse aspect ratio  $\lambda = \frac{\omega_z}{\omega_\rho}$  in the equation for the full dispersion relation. We also use that  $\tau = \frac{5}{4\gamma_{coll}}$  and  $\tilde{\gamma} = \frac{\gamma_{coll}}{\omega_z}$ . Then we write [6]

$$\begin{aligned} \omega_q(\omega_q^2 - 4\omega_z^2)(\omega_q^2 - 4\omega_\rho^2) - \frac{i}{\tau}[\omega_q^4 - \frac{2}{3}\omega_q^2(5\omega_\rho^2 + 4\omega_z^2) + 8\omega_\rho^2\omega_z^2] &= 0 \\ \omega_z^4(\omega_t^2 - 4)(\omega_t^2 - 4\lambda^{-2}) - \frac{i}{\omega_t\omega_z\tau}\omega_z^4[\omega_t^4 - \frac{2}{3}\omega_t^2(5\lambda^{-2} + 4) + 8\lambda^{-2}] &= 0 \\ \omega_t(\omega_t^2 - 4)(\omega_t^2 - 4\lambda^{-2}) - \frac{i}{\omega_z\tau}[\omega_t^4 - \frac{2}{3}\omega_t^2(5\lambda^{-2} + 4) + 8\lambda^{-2}] &= 0 \\ \omega_t(\omega_t^2 - 4)(\omega_t^2 - 4\lambda^{-2}) - i\frac{4\gamma}{5\omega_z}[\omega_t^4 - \frac{2}{3}\omega_t^2(5\lambda^{-2} + 4) + 8\lambda^{-2}] &= 0 \\ \omega_t(\omega_t^2 - 4)(\omega_t^2 - 4\lambda^{-2}) - i\frac{4}{5}\tilde{\gamma}[\omega_t^4 - \frac{2}{3}\omega_t^2(5\lambda^{-2} + 4) + 8\lambda^{-2}] &= 0 \end{aligned}$$

After rewriting in this manner we see that our equation is only dependent on the hydrodynamicity and the inverse aspect ratio. To make the solution more insightful we expand it

$$\omega_t^5 - i\frac{4}{5}\tilde{\gamma}\omega_t^4 - 4(\lambda^{-2} + 1)\omega_t^3 + i\frac{8}{15}\tilde{\gamma}(5\lambda^{-2} + 4)\omega_t^2 + 16\lambda^{-2}\omega_t - i\frac{32}{5}\tilde{\gamma}\lambda^{-2} = 0 \quad (25)$$

and observe that this is a fifth order equation for the complex variable  $\omega_t$ . The physical interpretation of the possibility that  $\omega_t$  can be complex is that there may be damping of the quadrupole modes involved. This is not a possibility for the previous cases, the collisionless regime and the hydrodynamic regime, where the solutions were real. We therefore define

$$\omega_t = \omega + iT \quad (26)$$



It is convenient to define the pre-factors in Equation (25) in six new parameters

$$\begin{aligned}\beta_5 &= 1 & \beta_4 &= -\frac{4}{5}\tilde{\gamma} & \beta_3 &= -4(\lambda^{-2} + 1) \\ \beta_2 &= \frac{8}{15}\tilde{\gamma}(5\lambda^{-2} + 4) & \beta_1 &= 16\lambda^{-2} & \beta_0 &= -\frac{32}{5}\tilde{\gamma}\lambda^{-2}\end{aligned}$$

so that we obtain an equation that is more easy on the eyes.

$$\beta_5\omega_t^5 + i\beta_4\omega_t^4 + \beta_3\omega_t^3 + i\beta_2\omega_t^2 + \beta_1\omega_t + i\beta_0 \quad (27)$$

We can solve this equation by requiring the imaginary and real part to vanish separately. This allows us to write our equation for a complex variable into two coupled real equations which are solved with relative ease by existing algorithms. The definition  $\omega_t = \omega + iT$  is then inserted giving us

$$\begin{aligned}\beta_1\omega - 2\beta_2T\omega - 3\beta_3T^2\omega + 4\beta_4T^3\omega + \beta_3\omega^3 - 4\beta_4T\omega^3 - 10\beta_5T^2\omega^3 + \beta_5\omega^5 + \\ i(\beta_0 + \beta_1T - \beta_2T^2 - \beta_3T^3 + \beta_4T^4 + \beta_5T^5 + \beta_2\omega^2 + 3\beta_3T\omega^2 - 6\beta_4T^2\omega^2 - 10\beta_5T^3\omega^2 + \\ \beta_4\omega^4 + 5\beta_5T\omega^4)\end{aligned} \quad (28)$$

We can numerically solve this by typing a code in mathematica [6]. It can be checked in Figure 5. The code returns five predicted values for  $\omega_t$  for every  $\lambda$  and  $\tilde{\gamma}$ . One is zero which is trivial and the other four are  $\pm\omega_t$ . The negative modes are unphysical solutions. The code also predicts a nonzero value for the damping parameter  $T$  when the system is in the intermediate regime.

```

Qpole[λ_, γ_] := Module[{b0, b1, b2, b3, b4, b5, realpart, imagpart, w, t},
  b5 = 1; b4 =  $\frac{-4 \gamma}{5}$ ; b3 =  $-4 (\lambda^{-2} + 1)$ ; b2 =  $\frac{8 \gamma}{15} (5 \lambda^{-2} + 4)$ ; b1 =  $16 \lambda^{-2}$ ; b0 =  $\frac{-32}{5} \gamma \lambda^{-2}$ ;
  realpart = b1 w - 2 b2 t w - 3 b3 t^2 w + 4 b4 t^3 w + 5 b5 t^4 w + b3 w^3 - 4 b4 t w^3
    - 10 b5 t^2 w^3 + b5 w^5;
  imagpart = b0 + b1 t - b2 t^2 - b3 t^3 + b4 t^4 + b5 t^5 + b2 w^2 + 3 b3 t w^2 - 6 b4 t^2 w^2
    - 10 b5 t^3 w^2 + b4 w^4 + 5 b5 t w^4;
  sol = NSolve[{realpart == 0, imagpart == 0}, {w, t}, Reals, WorkingPrecision -> 50];
  w = w /. sol;
  t = t /. sol;
  {w, t, {λ, γ}/1.}]

```

**Figure 5:** The mathematica code used for calculating  $\omega_t$  in the intermediate regime

It is now possible to take a look at the transition from the collisionless case (crossing) to the hydrodynamic case (avoided crossing) by varying  $\tilde{\gamma}$ . A graph with  $\tilde{\gamma} = 1.8$  is depicted below.

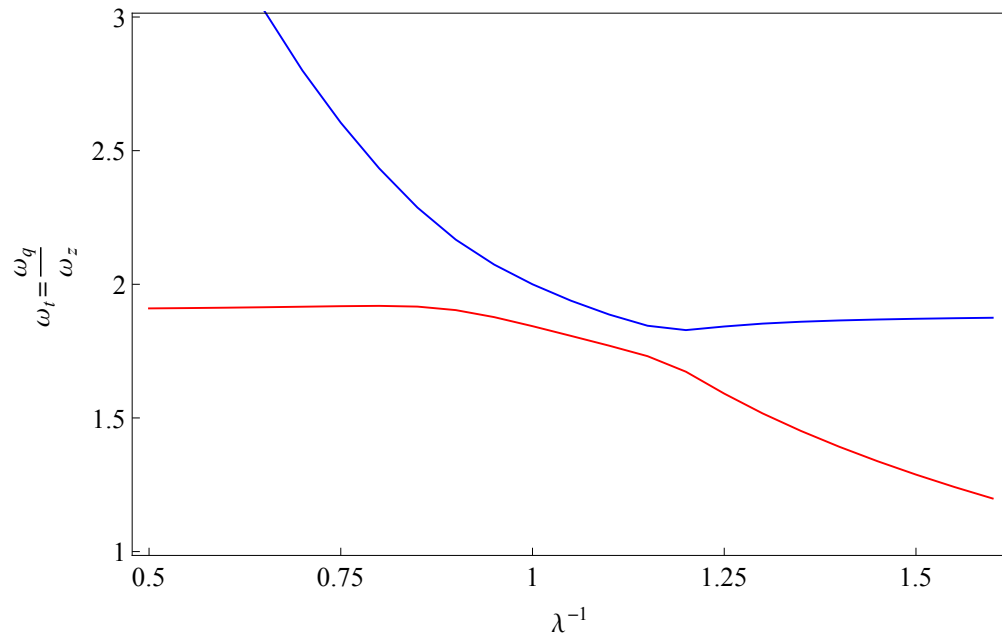


**Figure 6:** We observe a graph that is somewhere in the middle between the two previous cases. In this case  $\tilde{\gamma} = 1.8$ . An avoided crossing is still present.

The avoided crossing is always present but becomes smaller and smaller for decreasing  $\tilde{\gamma}$ . The crossing is reobtained for  $\tilde{\gamma} = 0$ . For  $\tilde{\gamma} \geq 5$  the avoided crossing is almost identical to the fully hydrodynamic case.

### 3 Experiment

Our experiment will start with a thermal cloud at rest trapped inside a harmonic magnetic potential. Because it is at rest its aspect ratio will not vary. It is then perturbed by ramping up either  $\omega_z$  or  $\omega_\rho$  in a time frame of 20 ms. The strength of the perturbation is expressed as  $\frac{\Delta\omega}{\omega}$ . If this value is chosen too small it will get extra difficult or impossible to measure the responding quadrupole oscillation. If you choose it too high however the cloud may give a non-linear response which is undesirable as well. After the kick (which the perturbation is often referred to) there is a waiting period of typically another 20 ms. Subsequently the cloud is imaged at regularly spaced intervals, depending on the desires of the experimentalist somewhere between 5 and 20 ms. If these intervals are too long, such that there are less than 2 images per period of  $\omega_q$ , we can no longer find the correct value for  $\omega_q$ . We can shorten the imaging intervals when we expect a large value for  $\omega_q$ . With our experimental setup it is feasible to create clouds with an inverse aspect ratio varying from 0.11 to 1.6.

#### 3.1 Measuring

After the perturbation the cloud will begin to oscillate in two different ways. The first is the quadrupole mode we wanted to excite. The second is an ordinary dipole oscillation, the movement of the center of mass of the cloud. The latter will turn out to be useful in measuring the used trap frequencies.

The cloud is then, while it is oscillating, photographed by using non-destructive phase-contrast imaging. This is an imaging technique that bombards the cloud with a coherent bundle of photons. The difference in refractive index between the sodium cloud and the surrounding vacuum results in an acquired phase difference.

This can be measured with a small, flat lightsensitive sensor consisting of around half a million pixels. Thereby a picture of the cloud is created (see Figure 7). Moreover the cloud is not instantly evaporated by this imaging method. This makes it ideal to make multiple pictures of one cloud at different moments in the evolution of it's movement. A single cloud is typically imaged 30 to 50 times with 20 ms between each image. When we look at these images in sequence we see a short movie of the evolution of the aspect ratio in time.

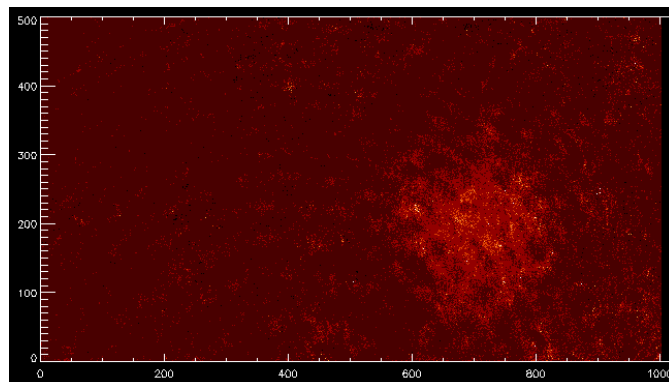


**Figure 7:** An image of a thermal cloud made with non-destructive phase-contrast imaging. A consecutive series of these pictures make up a movie.

The next step is to objectively measure the shape of the cloud  $\lambda$  from the images. For this purpose an excellent program was written by Thomas Berlok called Run-Analysis.Pro [6] which can be found on the server. This IDL-routine attempts to fit a 2D Gaussian profile to the image that has the following form

$$p_0 * \text{Exp}\left[-\frac{(\text{Cos}[p_5] * (x - p_1) - \text{Sin}[p_5] * (y - p_2))^2}{2 * p_3^2} - \frac{(\text{Sin}[p_5] * (x - p_1) - \text{Cos}[p_5] * (y - p_2))^2}{2 * p_4^2}\right] + p_6 \quad (29)$$

The subscripted p's are the fitting parameters.  $p_0$  is the amplitude,  $p_1$  and  $p_2$  the position in the x and y direction respectively.  $p_3$  and  $p_4$  represent the length and width of the cloud.  $p_5$  is the angle and  $p_6$  is the elevation of the Gaussian profile above zero. The physical interpretation of this parameter is a measure for the background-noise. A fit to the image shown before is depicted in Figure 8. The

fitted parameters are saved in a .dat file and stored on the server.

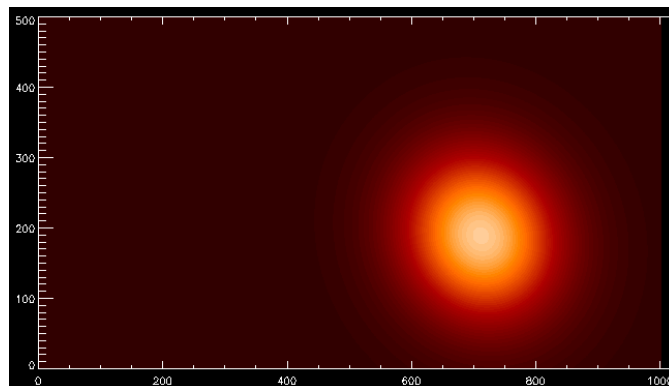


**Figure 8:** The fit of Equation 31 to Figure 7

There are however some serious issues with the acquired information as was discovered after initial confusion. The program was initially written for a purpose that assumed the thermal cloud not to be in the vicinity of  $\lambda = 1$ . We however are especially interested in this region and were using the program for such purpose. This works fine until you take a good look at the data lists for  $\sigma_z$  and  $\sigma_\rho$ . You will discover that in about fifty percent of the cases the correct value for the width is interchanged with the value for the length. This makes further analysis futile. In the beginning it is hard enough even to recognize this problem because the values for length and width are close together.

As always the solution starts with understanding the problem. It is my understanding that the problem arises because a quadrupole mode in the vicinity of  $\lambda = 1$  continuously changes what the longest axis of the cloud is. The program seems to store the longest axis usually in one list and the shortest axis in the other. This is not what you want though. You want the axis in the z-direction always stored in one list and the perpendicular axis in the second list independent of it being the shortest or the longest axis.

The above is not a hard rule though, not all the largest values are stored in one list. After some more thinking and the help of my superiors it was recognized that

the program misinterpreted the changing of which axis was the longest, due to the quadrupole mode, as a  $90^\circ$  rotation of the entire cloud. As can be seen in Equation (29) the angle of the cloud is a degree of freedom in the fitting procedure. It was then tried to fix the angle parameter at a constant that was visually checked to be approximately equal to the orientation of the cloud. However, as a result of the initial kick, the angle of the cloud is not constant but oscillating around its equilibrium position with an amplitude of around  $\pm 15^\circ$ . This makes fixing the angle parameter not ideal because the rotation then distorts the measurement for the length and width. Because the result we are looking for is already not evident in the data this extra error would make it near impossible to detect.

The best way to regain the correct results in the correct lists was eventually found in the  $90^\circ$  rotation that the program thought occurred when the longest axes changed. First, in the fitting procedure, the angle was no longer fixed to a constant. Then, when you plot the values for the angle, you see that you get values exceeding  $2\pi$  ( $10\pi$  was observed). This is a remnant of the fitting procedure that rotates the Gaussian profile a number of times in an attempt to find the best fit. It sounds logical that the number of rotations gets higher as the aspect ratio gets closer to one because finding an angle becomes increasingly difficult for rounder objects. Limiting the maximum rotation-angle in the program was not an option because this often resulted in wrong angles.

For every found angle you have to take the value  $\theta \text{Mod} \pi$  such that a value between 0 and  $\pi$  remains. When you look at this new plot of angles you observe different plateaus with approximately  $\frac{1}{2}\pi$  or  $90^\circ$  between them. For all the values that turned  $90^\circ$  with respect to the first value you have to interchange the corresponding width and length. In this way it is possible to regain the correct results. Even though this is labor-intensive the author could not find another way and frankly was happy that this seemed to work.

## 3.2 Analysis

We start our analysis at the dipole mode. The center of mass of the cloud will tend to oscillate with the same frequency as the trap frequencies. Measuring the dipole modes is thus an excellent way to acquire  $\omega_z$  and  $\omega_\rho$ . We plot the 30 to 50 different values for  $p_1$  and  $p_2$  in a graph and try to fit a simple damped periodic function like

$$e^{-\alpha t} * A * \text{Sin}[\omega_z t + \phi] + d \quad (30)$$

The best fit is easily found with for instance Mathematica. We show an example of a fit to the axial movement of a cloud with  $\lambda = 1$  in Figure 9.

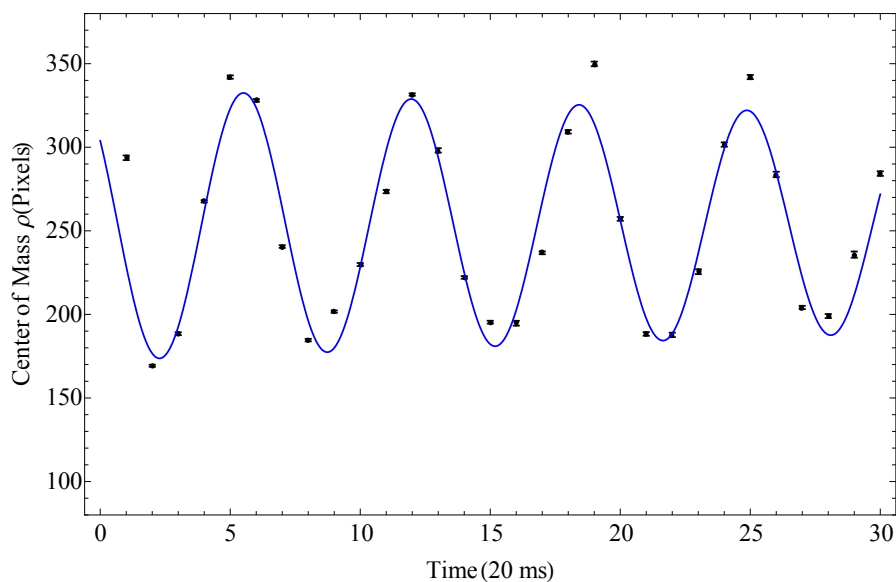


**Figure 9:** Fit to the axial movement of a cloud with  $\lambda = 1$

When  $\omega_z$  and  $\omega_\rho$  are known we immediately know the aspect ratio. We then only need the number of particles  $N$  to calculate the hydrodynamicity. We do not necessarily need the temperature for this because we can rewrite Equation 18 into

$$\tilde{\gamma} = \frac{N\sigma_0}{2\pi^2\sigma_\rho^2} \quad (31)$$

We can estimate the number of particles in the cloud by multiplying the length, width and amplitude of the Gaussian distribution. There is however a conversion factor  $C$  involved that is related to how much phase difference the radiation accumulates while passing through a section of the cloud with optical column depth  $\rho_c$

$$N = CA\sigma_\rho\sigma_z \quad (32)$$

Here  $C$  is a conversion factor. A plot of the number of particles from a cloud is pictured in Figure 10.

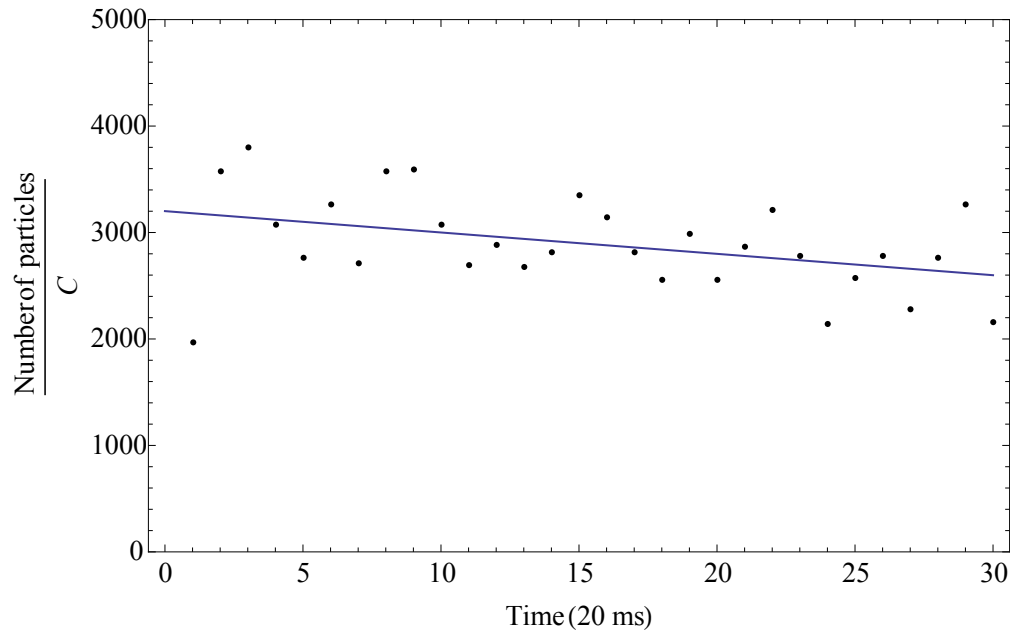


**Figure 10:** The number of particles in a thermal cloud as a function of time.

It is clearly visible that  $N$  decreases as a function of time. This is a remnant of the phase-contrast imaging. Although it is non-destructive we still lose some atoms due to the probe beam. It has been shown by Koller that higher beam intensity



results in faster loss of atoms [1].

We can calculate the number of particles by a different route such that we can find C. We consider the relation between the amplitude of the Gaussian profile and the optical column depth of the cloud. It takes the following form

$$\phi = \pi \frac{Re(\alpha)}{\epsilon_0 \lambda} \rho_c \quad (33)$$

Here,  $\lambda$  is the wavelength of the probe radiation and  $\alpha$  is an expression for the complex polarizability

$$\alpha = \frac{ic\epsilon_0\sigma_\lambda}{\omega} \sum_e \frac{D_{F_e}(\beta)}{1 - 2i\delta_e/\gamma} \quad (34)$$

With  $\omega$  the frequency for the atomic transitions and  $\sigma$  being the cross section

$$\sigma_\lambda = \frac{3\lambda^2}{2\pi} \quad (35)$$

Furthermore

$$\begin{aligned} D_0(\beta) &= \frac{4}{24} \sin^2[\beta] \\ D_1(\beta) &= \frac{5}{24} (1 + \cos^2[\beta]) \\ D_2(\beta) &= \frac{6}{24} + \frac{1}{24} \sin^2[\beta] \end{aligned}$$

In these equations  $\beta$  is the angle. The dependence on the angle is negligible for probe frequencies close to resonance. This condition is satisfied in our case for we use a detuning of  $\delta = -4 * 99.9$  MHz. Out of the optical column depth we can then calculate N and thus C.

By using Equation 31 we can now calculate  $\tilde{\gamma}$  for arbitrary aspect ratio, provided we know  $N$ . We did this for  $\lambda^{-1} = 0.78$ ,  $\lambda^{-1} = 1$  and  $\lambda^{-1} = 1.21$ . The results are respectively  $\tilde{\gamma} = 0.06$ ,  $\tilde{\gamma} = 0.04$  and  $\tilde{\gamma} = 0.11$ .

These values are very low when we compare them to the discussion about the intermediate regime in section 2.3. This means that the avoided crossing will be almost impossible to measure. When we take another look at Equation 31 we observe that it is proportional to the number of particles and inversely proportional to the square of the width in the radial direction. For clouds with the same number of particles a pancake-like shape therefore has a far smaller  $\tilde{\gamma}$  than a cigar shaped cloud. An almost spherical cloud will be somewhere in the middle. Because we are only interested in spherical clouds changing the shape to increase  $\tilde{\gamma}$  is no option. We are thus limited by the number of particles which is limited by the experimental setup. Higher hydrodynamicities are as yet not possible for this reason.

We are now in the position to measure the  $\omega_q$ 's and compare them with the predicted values from the mathematica code. We thus attempt to make a fit to  $\sigma_z$  and  $\sigma_\rho$ . Both quadrupole frequencies can be detected in just one of these dimensions. This is because the two modes influence one another due to the atoms colliding in the cloud. It is of course preferable to measure both values for  $\omega_q$  in  $\sigma_z$  as well as in  $\sigma_\rho$  for comparison. The fastest way to do this is to make the fit to  $\lambda = \frac{\omega_z}{\omega_\rho}$ . Therefore we attempt to fit a damped double sine-function to the aspect ratio

$$e^{-\alpha * t} * A * \text{Sin}[\omega_z t + \phi_1] * \text{Sin}[\omega_\rho t + \phi_2] + d \quad (36)$$

A graph of a typical fit is shown in Figure 11.

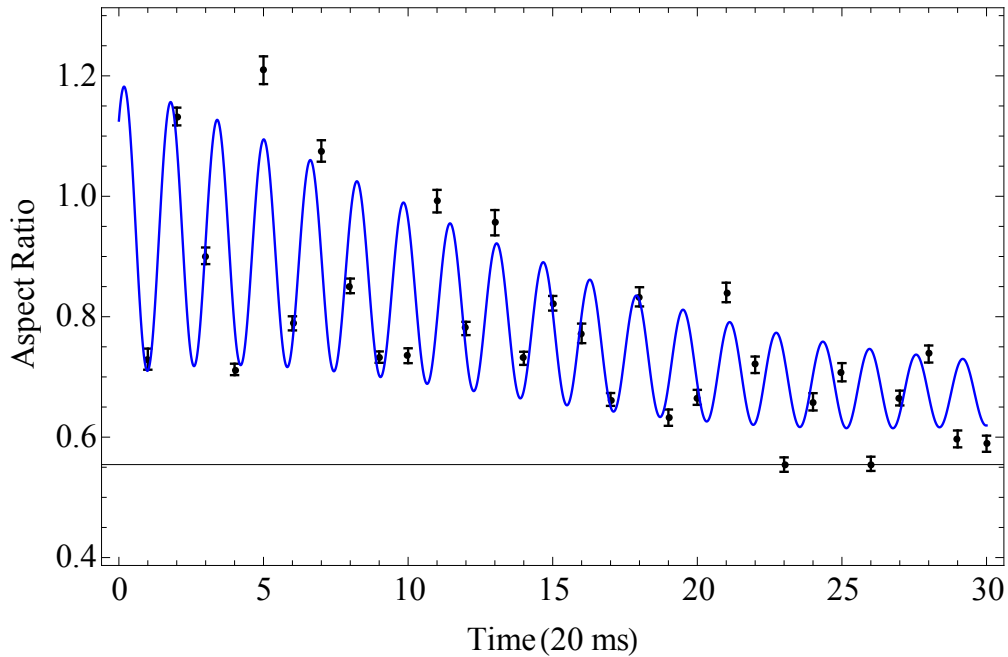


**Figure 11:** A typical fit to the aspect ratio. Goodness of Fit is 0.96

Finding this fit is far from trivial. Mathematica has serious trouble with finding the best fit. My initial approach was to continuously change the starting values in the NonlinearModelFit and/or put constraints on the possible parameter values. The quality of the fit was then judged by a Pearson Goodness of Fit test. This process is repeated until it was believed no better fit existed or could be acquired by said method. It may be clear that this method is far from ideal.

What is actually needed for this kind of problem is a genetic algorithm. I have started putting together a C-routine for this purpose. Writing a genetic algorithm is timeconsuming and I did not finish it in time to use it myself. It is near completion though. In principle all the basic elements are present. You can compile and run the program after which it will open a console that shows the fitness of every generation. It does not however print the actual answer to the problem. How this is done is something that is still unclear to me. I used the very simple problem  $x^2 - 3x - 1.56 = 0$  so the next step will be implementing your own specific optimization problem. The program is called GeneticAlgorithm.c and you can open it

with the program DEV-C++.

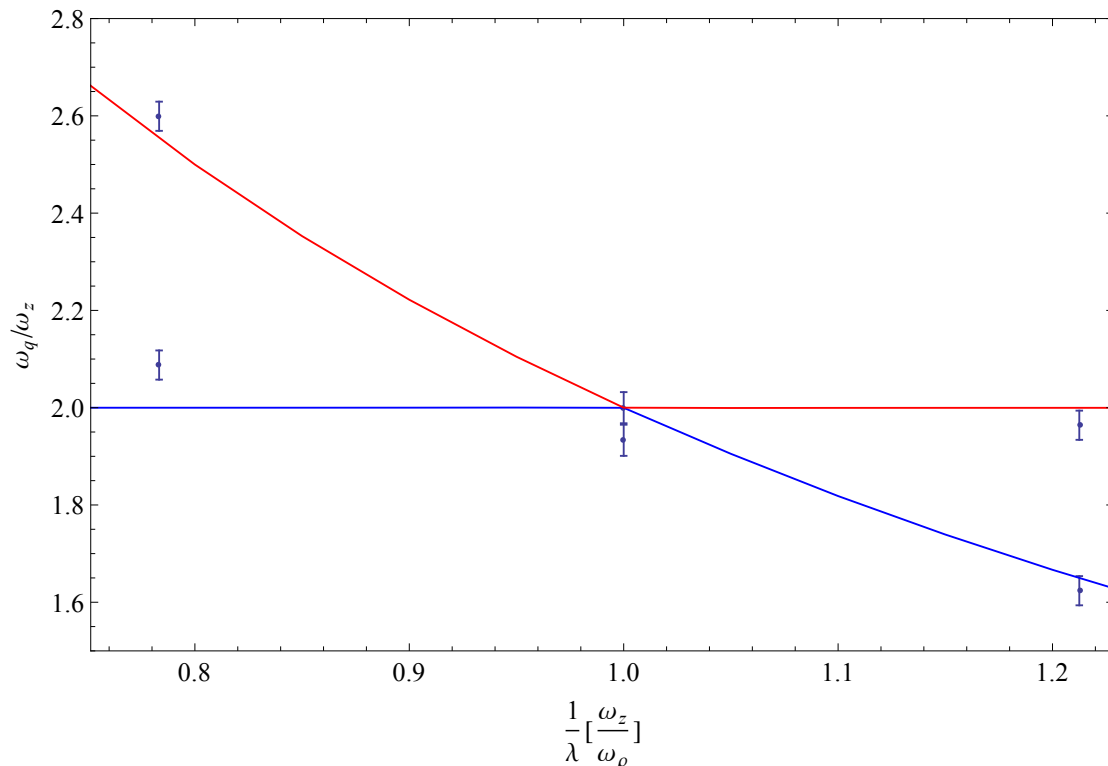


**Figure 12:** Comparison of measured  $\omega_q$  with the theoretical values for three different aspect ratios

In this graph we indicated the predictions with a blue and red line. These are the result of the numerical calculations with Qpole where we used a hydrodynamicity of 0.07. The measurements actually had three different values for  $\tilde{\gamma}$ , namely 0.04, 0.06 and 0.11. These hydrodynamicities are so low though that there is no observable difference between the quadrupole curves when we plot them and we can approximate them with the single value of 0.07. This makes it possible to plot the prediction as a curve instead of a single point for every measurement which is more pleasing to the eye. We observe a good correspondence between measurements and theory. Due to the uncertainties it is not possible to detect an avoided crossing if it is present. The very low hydrodynamicities stated above made this very unlikely to begin with. To have a serious chance of detecting an avoided crossing the

number of particles needs to be at least one order of magnitude higher with the dimensions of the cloud unchanged. Because this increases the density 10-fold this will also lead to an increase in the loss of particles due to 3-body collisions. What the net result for  $\tilde{\gamma}$  will be cannot be easily calculated. When we keep in mind that our BEC-setup is able to produce condensates with the highest number of atoms in the world I conclude that the avoided crossing is unlikely to be measured in the foreseeable future.

## References

- [1] Silvio B. Koller. *Experiments on Hydrodynamic Transport in Ultra-Cold Bose Gases*. 2012: Utrecht University.
- [2] A. Griffin, Wen-Chin Wu, and S. Stringari. *Hydrodynamic Modes in a Trapped Bose Gas above the Bose-Einstein Transition*. Physical Review Letters, 78(10), 1997.
- [3] David Gury-Odelin, Francesca Zambelli, Jean Dalibard, and Sandro Stringari. *Collective oscillations of a classical gas confined in harmonic traps*. Physical Review A, 60(6), 1999.
- [4] U. Al Khawaja, C. J. Pethick, and H. Smith. *Kinetic Theory of Collective Modes in Atomic Clouds Above the Bose-Einstein Transition Temperature*. Journal of Low Temperature Physics, 118, 2000.
- [5] W. Ketterle, D.S. Durfee, and D.M. Stamper-Kurn, editors. *Making, probing and understanding Bose-Einstein condensates*, 1999.
- [6] T. Berlok. *Quadrupole oscillations of hydrodynamic Bose gases*. 2013: Utrecht University